Supplemental Figures

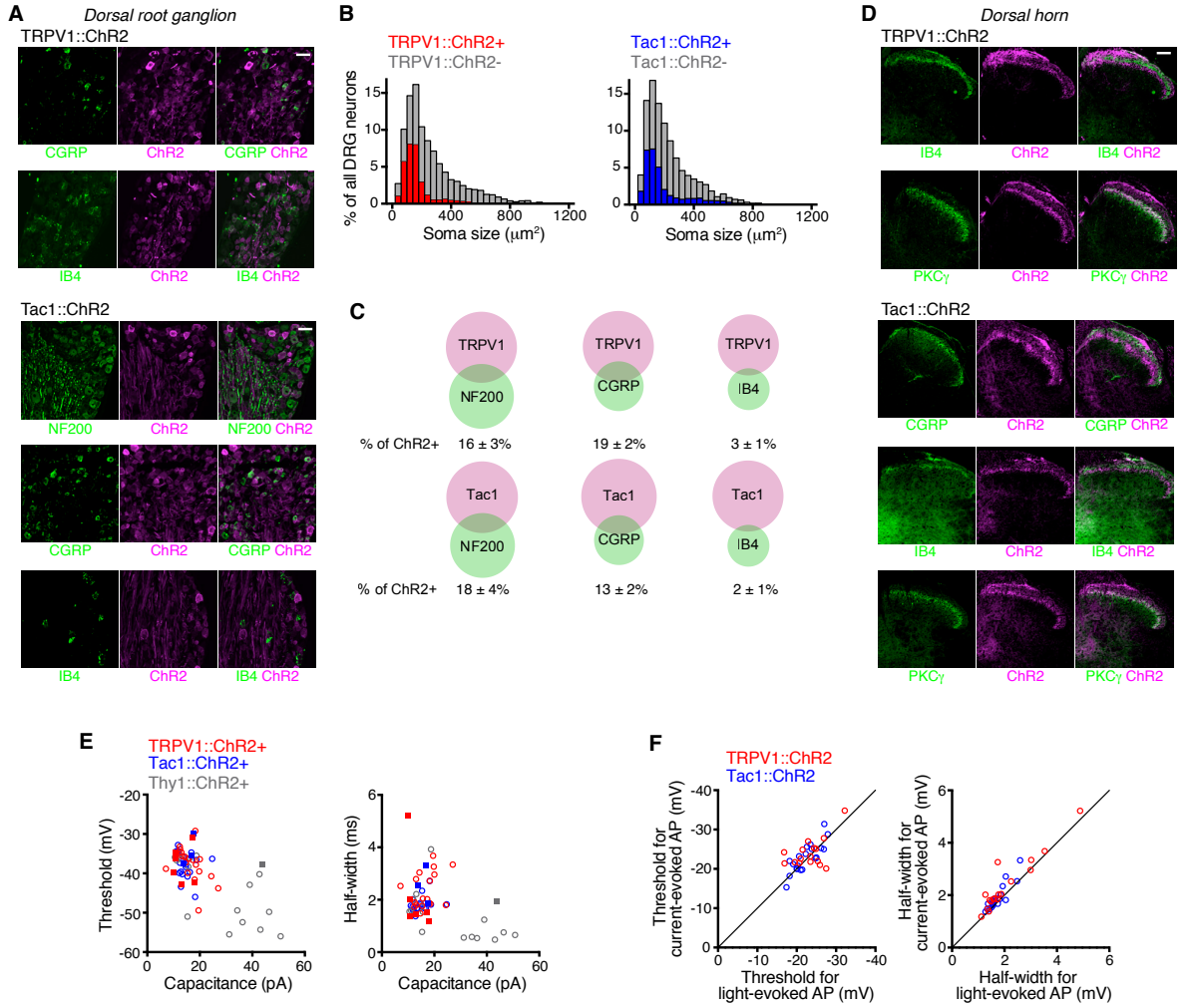

Figure S1. Expression of ChR2 in cutaneous nociceptors, related to Figure 1. (A) Expression of ChR2 in the dorsal root ganglion. Tissue from TRPV1::ChR2 and Tac1::ChR2 mice stained for CGRP (for peptidergic neurons), IB4 (for non-peptidergic neurons) and NF200 (for myelinated neurons). Scale bar represents 20 μm. (B) ChR2 is predominantly expressed in small-diameter DRG neurons. Distributions of neuron size measured in immunostained (NeuN) fixed DRG tissues (L3-L5). ChR2+ neurons were identified by the presence of tdTomato fluorescence. Tissues were obtained from four mice for each genotype, from which 3379 neurons were measured for TRPV1::ChR2 (left) and 2538 neurons for Tac1::ChR2 (right). (C) ChR2 is expressed in neurons that match nociceptor profiles. Fixed DRG tissues (L3-L5) were stained and ChR2+ neurons identifed by the presence of tdTomato fluorescence. Neurons were counted for ChR2+ and NF200+ (TRPV1::ChR2 = 2384 total; Tac1::ChR2 = 1709 total), ChR2+ and CGRP+ (TRPV1::ChR2 = 1609 total; Tac1::ChR2 = 911 total), and ChR2+ and IB4+ (TRPV1::ChR2 = 1778 total; Tac1::ChR2 = 1203 total). Four mice were used for each genotype. Data are indicated as mean ± SEM. (D) Expression of ChR2 in primary afferent nociceptors that project into the superficial lamina of the dorsal horn spinal cord. Tissue from TRPV1::ChR2 and Tac1::ChR2 mice stained for CGRP (for lamina I-II outer), IB4 (for lamina II inner) and PKCγ (for lamina II-III). Some Tac1:ChR2+ fibres terminated in deeper lamina of the spinal cord. Scale bar represents 20 μm. (E) Representative whole-cell patch clamp recordings of cultured DRG neurons from Thy1::ChR2 mice. Thy1::ChR2 represent a mixed population of small and large diameter neurons. A 3 ms light pulse only ever generated single action potentials in Thy1::ChR2+ neurons and these with high- and low- threshold. TRPV1::ChR2 and Tac1::ChR2 recordings are shown in Fig. 1. (F) Action potentials evoked in cultured DRG neurons by injecting current at rheobase. Neurons that also responded to capsaicin (1 μM) are shown in square symbols. (G) Action potential properties were identical whether evoked by optogenetic stimulation or current injection. Action potentials were measured in current clamp mode of the whole-cell patch clamp technique, by injecting current at rheobase or applying a pulse of light (3 ms) in the same cell. Threshold (left) was significantly correlated between light-evoked and current-evoked action potentials (TRPV1, n = 17, $p = 0.013$; Tac1, n = 20, $p < 0.0001$). This was also the case for half-width (right) (TRPV1, n = 17, $p < 0.0001$; Tac1, n = 20, $p < 0.0001$).

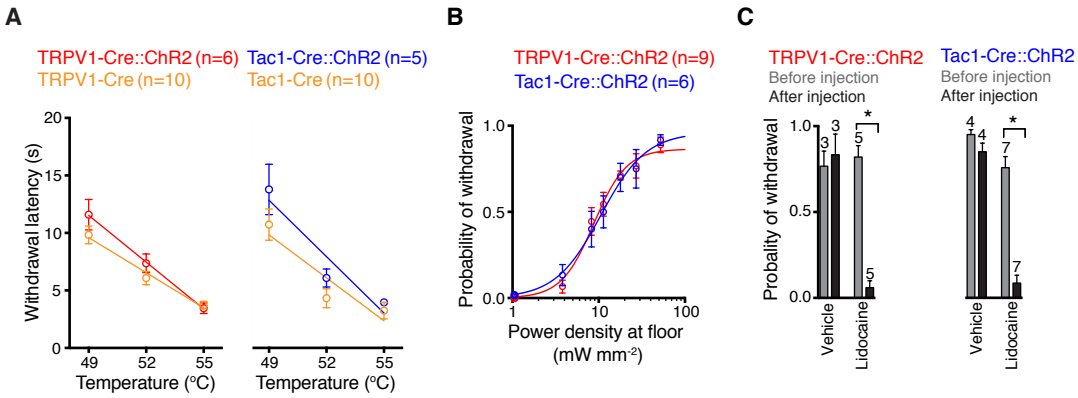

Figure S2. Sensitivity to noxious thermal cutaneous stimuli and specific optogenetic activation of afferent fibers, related to Figure 1. (A) Hotplate assay for thermal sensitivity. TRPV1-Cre::ChR2 and Tac1-Cre::ChR2 mice are shown alongside controls. (B) Light-evoked hindpaw withdrawal was dependent on light intensity. Hindpaw withdrawal was counted over ten trials of light (10 ms) applied at each power density. It is important to note that littermate controls without Cre recombinase, or without ChR2, never reacted to a 10 ms blue light pulse (15 mice, 3 trails each). TRPV1::ChR2 and Tac1::ChR2 mice did not respond to an equivalent off-spectra pulse of light (594 nm, three trials in seven mice each for TRPV1::ChR2 and Tac1::ChR2). (C) Light-evoked withdrawal was attenuated by locally delivered lidocaine indicating that electrical activity in paw afferents was responsible. Intraplantar injection of lidocaine in PBS (2%, 20 ul) into the left hindpaw 5-10 minutes before counting hindpaw withdrawals in reponse to light (10 ms, 25 $mW.mm^{-2}$, ten trials >1 minute apart). Numbers of mice are shown. Data are represented as mean ± SEM. * = $p < 0.001$ (Student's t-test).

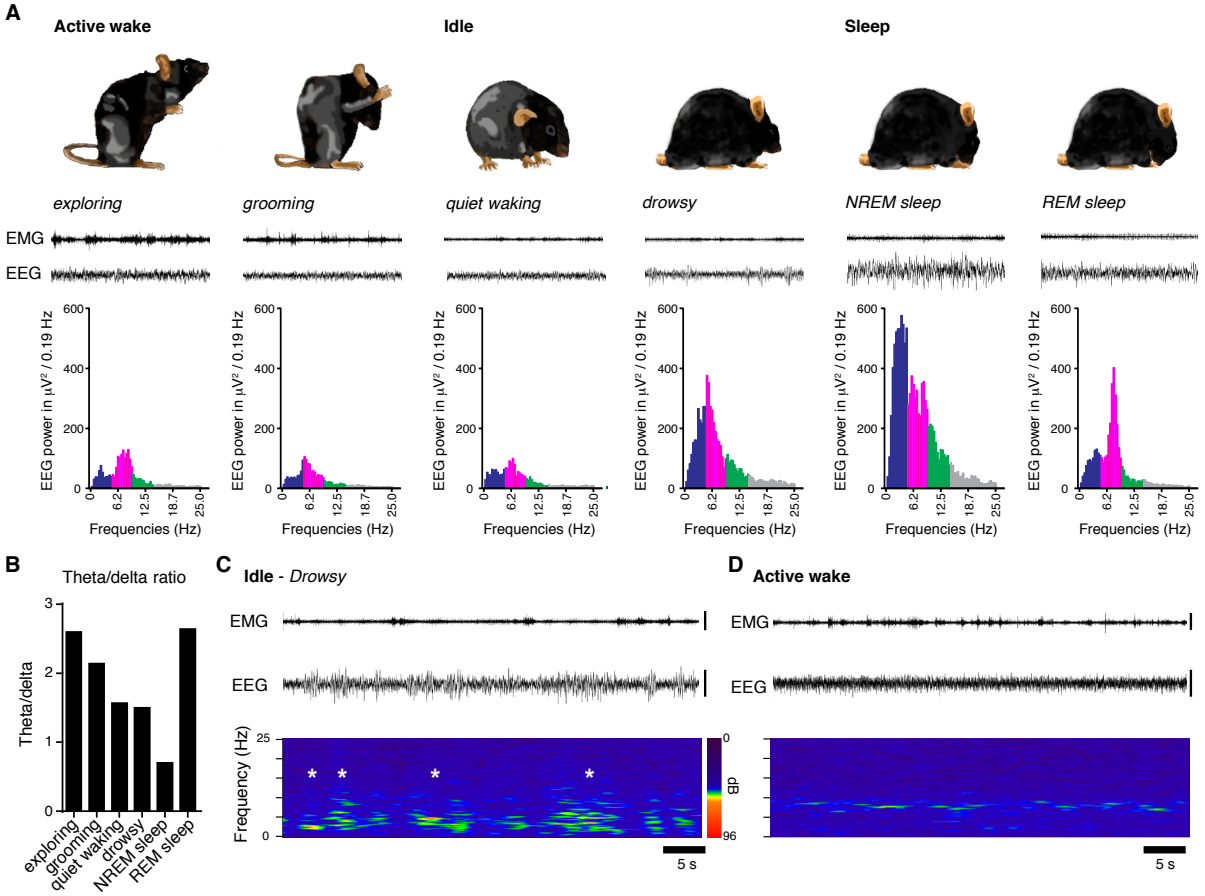

Figure S3. Cortical EEG recordings across different behavioral states, related to Figures 3 to 5. (A) Examples of different behavioral states in the mouse from active waking (left) to sleep (right). For each behavioral state, top to bottom: illustrative cartoon, representative electromyogram (EMG) and electroencephalogram (EEG) signal traces (60 s), and associated EEG power density spectra showing changes in various frequency bands across behaviors. Frequency bands: delta (blue, 0.5-5 Hz), theta (magenta, 5-9 Hz), alpha (green, 9-15 Hz), beta (grey, 15-25 Hz). During active wake such as exploration, power in the EEG shows an increase in the theta range (especially high theta around 8-9 Hz), while during quiet wake, EEG power peaks in the lower theta frequencies (5-6 Hz). NREM sleep is characterized by synchronous high amplitude slow waves also called delta "waves" (0.5-5 Hz), which amplitude correlates with sleep depth, and by spindle oscillations in the alpha range (11-15 Hz). Idle behaviors, such as quiet waking and drowsiness, show a gradual increase in EEG power within the delta and alpha ranges, and can ultimately result in a full transition to NREM sleep. REM sleep is characterized by both muscle atonia and prominent EEG activity in the high theta range. (B) EEG theta/delta ratio for each behavioral state. Idle states (quiet waking and drowsy) display similar ratio. (C) Example of a drowsy state with the occurrence of several bursts of sleep as shown by intrusion of delta waves in the EEG trace and greater EEG power in the delta range. Top, EMG and EEG traces (60 s). Bottom, heatmap representation of corresponding EEG power spectrogram (0-25 Hz). * indicate bursts of sleep. (D) Example of an active state: top, EMG and EEG traces, bottom, corresponding EEG power spectrogram (0-25 Hz). Exploration and active wake are characterized by intense EEG power at ~ 8 Hz (theta band), but very low power in the delta range. For all EMG and EEG traces, scale bars: 500 µV.

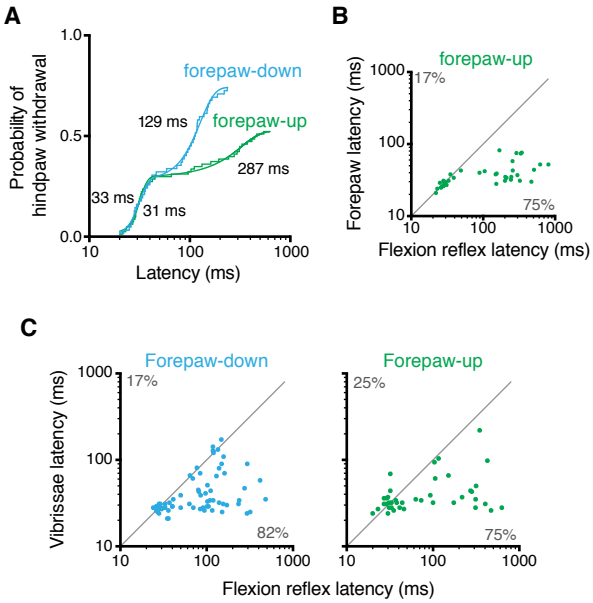

Figure S4. Optogenetically-evoked latencies from Tac1::ChR2 mice, related to Figures 3 and 4. (A) Cumulative density function for awake idle Tac1::ChR2 mice in forepaw-down (46 trials) or forepaw-up (42 trials) states where latency was measured from a 3 ms hindpaw stimulation. Mean values for each population are shown. (B) Latency for hindpaw withdrawal plotted against the latency for forepaw movement. (C) Relative timings for hindpaw withdrawal and vibrissae movement in awake idle Tac1::ChR2 mice. Latencies were measured from a 3 ms hindpaw stimulation in forepaw-down (left) or forepaw-up (right) states.

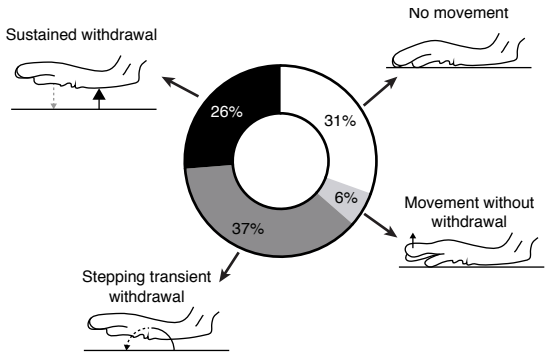

Figure S5. Nature and extent of hindpaw movement, related to Figure 3. The precise nature and extent of the hindpaw withdrawal response varied between trials. For example, responses in TRPV1::ChR2 mice ranged from no movement (36/118), paw movement without withdrawal (7/118), and a withdrawal that was either transient (flicked up then down) (44/118) or sustained (held off ground) (31/118), with on some occasions, a crossed extensor reflex (22/118). Sometimes an initial small movement of the hindpaw was observed well in advance of a delayed withdrawal (movement at 46 ± 8 ms, withdrawal at 220 ± 52 ms, Student's t-test $p = 0.008$, 6/118 recordings) suggesting that Aδ afferent information may on some occasions be received but not fully acted upon in terms of provoking withdrawal, which in these cases required a longer latency C-fiber input.

Supplemental Experimental Procedures

Mice

All mice were purchased from Jackson Laboratories. In addition to the TRPV1::ChR2 and Tac1::ChR2, ChR2-tdTomato was also expressed in a broader range of myelinated A-fiber neurons, by breeding Ai27D with Thy1-Cre mice (Dewachter et al., 2002) bred onto the C57BL/6j background for at least five generations.

Dorsal root ganglion neuron culture

Dorsal root ganglia neurons were isolated from adult (3-6 month old) mice and placed into cold Hank's balanced salt solution. The ganglia were then digested for 70 minutes at 37°C in 5 $mg.ml^{-1}$ collagenase and 1 $mg.ml^{-1}$ Dispase II (Sigma). Cells were washed and triturated and then centrifuged through 10% bovine serum albumin (vol/vol) in phosphate buffered saline. The cell pellet was resuspended in neurobasal A containing B27 supplement (L-glutamine (200 mM), 1% penicillin and streptomycin (10,000 $U.ml^{-1}$), NGF (50 $ng.ml^{-1}$) and GDNF (2 $ng.ml^{-1}$). Cells were seeded onto poly-D-lysine–coated (500 $\mu g.ml^{-1}$) and laminin-coated (5 $mg.ml^{-1}$) 12-mm borosilicate cover glasses (Fisher Scientific) in 35-mm dishes (Becton Dickinson) at 8,000–9,000 per dish. Cells were maintained at 37 °C in 5% carbon dioxide for up to 24 hours.

Thermal sensitivity

Thermal sensitivity was determined using the hotplate assay, where mice were placed onto a hotplate (Bioseb) set at 49 °C, 52 °C or 55 °C until nocifensive behavior was observed. The latency for the onset of nocifensive behavior was measured. Thermal sensitivity was not altered by the expression of ChR2 in cutaneous nociceptors (Figure S2A).

Immunohistochemistry

Mice were anesthetised with pentobarbital (100 $mg.kg^{-1}$ intraperioneal) and fixed by transcardial perfusion with 4% paraformaldehyde dissolved in phosphate buffered saline (PBS). The spinal lumbar enlargement, DRG (L3-L5), and skin from the hindpaw and tail were dissected, postfixed, washed, cryoprotected with sucrose in PBS (30% w/v) for 2-3 days, and frozen (O.C.T., Tissue-Tek). Cryosections of spinal cord (20 μm thick), DRG (10 μm thick) and skin (hindpaw, 40 μm thick; tail, 20 μm thick) were blocked with 1% bovine albumin serum and 0.1% triton X-100 in PBS for one hour. Sections were incubated with primary antibodies in fresh blocking solution overnight at 4°C and washed three times (10 minutes each) in PBS. They were then incubated with secondary antibodies for one hour at room temperature, washed three times (10 minutes each) in PBS, and mounted in Vectashield. Tissues were obtained from four TRPV1::ChR2 mice and four Tac1::ChR2 mice. Antibody dilutions were NF200, 1:2000; CGRP, 1:500; PKCγ, 1:2000; NeuN, 1:1000; and secondary IgG, 1:500. Fluorescein-conjugated GSL I was used at 1:1000.

Fluorescence imaging

Tissues from TRPV1:ChR2 and Tac1::ChR2 mice were examined (four mice for each genotype). ChR2-tdTomato was imaged in skin (from the plantar surface of the hindpaw and the distal tip of the tail) using a Zeiss laser-scanning confocal microscope (LSM 710). Excitation was performed with a DPSS laser (561 nm) through Zeiss Neofluar 40x, 1.30 N.A. oil objective (hindpaw skin) or Zeiss Plan-Apochromat 63x, 1.40 N.A. oil objective (tail skin) to generate a 40 μm thick volumes.

DRG and spinal cord sections were imaged using a Nikon Eclipse 80i microscope using a Nikon 10X objective and Nikon DS-Qi1MC camera. Three slides were imaged for each antibody, each containing tissues from multiple genotypes for purposes of comparison. Cell area was estimated in ChR2-tdTomato+ and NeuN+ cells. Images were analysed using ImageJ. In skin, DRG and spinal cord, fluorescence corresponding to tdTomato was absent in tissues from littermate mice that did not express ChR2-tdTomato, or that did not express Cre recombinase (n = 2 for each littermate control variant for each of the three Cre lines)

In vitro electrophysiology

Recordings were made at 20-22°C up to 24 h after DRG neuron dissociation, using the whole-cell configuration of the patch-clamp technique. Recording pipettes were pulled from thin-walled borosilicate glass capillaries (World Precision Instruments, Sarasota, FL) on a Sutter Instrument P-97 puller (Novato, CA) and fire polished to tip resistances of 4–8 MΩ when filled with (in mM): 135 K-gluconate, 10 KCl, 1 $MgCl_2$, 5 EGTA, and 10 HEPES, pH 7.3. The extracellular solution contained (mM): 145 NaCl, 5 KCl, 2 $CaCl_2$, 1 $MgCl_2$, 10 HEPES, and 10 glucose, pH 7.4. All solutions were maintained at 300–315 mOsm/l. Chemicals were purchased from Sigma-Aldrich (St. Louis, MO). Membrane potential was recorded in current-clamp mode with an Axopatch 200A amplifier and Digidata 1400A A/D interface using pClamp 10.2 software (Molecular Devices, Palo Alto, CA). The data were low-pass filtered at 5 kHz (4-pole Bessel filter) and sampled at 10 kHz. Compounds were applied through a Perfusion Pencil and ValveLink8.2 controlled rapid perfusion system (AutoMate, Berkeley, CA). Input resistance was typically >500 MΩ, and cells with resistances <200 MΩ were discarded. Care was taken to maintain membrane access resistance as low as possible (usually 3–7 MΩ and always less than 10 MΩ). Resting membrane potentials of DRG neurons were -64 ± 1 mV for TRPV1::ChR2 (28 cells from three mice), -64 ± 1 mV for Tac1::ChR2 (21 cells from three mice), and -67 ± 2 mV for Thy1::ChR2 (17 cells from three mice). The same 473 nm DPSS laser used in behavioral experiments was used to apply light through the microscope objective to apply a 3 ms pulse (6 $mW.mm^{-2}$) to patched neurons. An individual action potential (AP) was only ever observed in the 66 neurons recorded from TRPV1::ChR2 (AP in 21/28 neurons, depolarisation without AP in 7/28 neurons), Tac1::ChR2 (AP in 20/21 neurons, depolarisation without AP in 1/21 neurons) and Thy1::ChR2 (AP in 17/17 neurons). We still only observed a single action potential with a higher power 3 ms pulse (46 $mW.mm^{-2}$; 26, 21 and 18 recordings for TRPV1::ChR2, Tac1::ChR2 and Thy1::ChR2 respectively), or a 10 ms pulse at varying power (7 $mW.mm^{-2}$ or 57 $mW.mm^{-2}$: both 26, 21 and 18 recordings for TRPV1::ChR2, Tac1::ChR2 and Thy1::ChR2 respectively). ChR2-negative neurons from these mice did not show any effect of light (4 neurons for TRPV1 mice, 4 neurons for Tac1 mice and 6 neurons for Thy1 mice).

In vivo electrophysiology

In vivo cell-attached recordings (Bai et al., 2015) were performed on TRPV1::ChR2 or Tac1::ChR2 mice (homozygous for ChR2) anesthetized with isoflurane. Two to five days prior to the recording, a fluorescent label (CTB-488) was injected into the left hindpaw to label the subset of DRG neurons innervating the paw. Following surgical exposure of the L4 DRG, a patch pipette was targeted under visual control to tdTomato and CTB-488 positive neurons. Light stimuli (90-100 mW single pulse, 1-3 ms duration) were applied to the left hindpaw with 30 second intervals between trials. Latency values reported are the time between the start of the light pulse and the arrival of the action potential at the cell body. Conduction velocities were estimated by a distance between skin and soma of 40 mm.

Electroencephalogram and electromyogram recordings

Mice were deeply anesthetized with isoflurane (3% induction, 2% maintenance) and placed in a stereotaxic apparatus (David Kopf Instruments). Four stainless steel screws were implanted for fronto-parietal EEG recordings (2.0 mm lateral to the right of the sagittal suture, 1.5 mm anterior to bregma, and 2 mm anterior to lambda). Two flexible EMG electrodes (multi-stranded stainless steel wire, AS131; Cooner Wire) were inserted into the neck extensor muscles. All electrodes were attached to a 2 x 3 micro-strip connector affixed to the animal's head with dental cement and the scalp wound was closed with surgical sutures. Mice were given meloxicam (5 mg/kg, i.p.) before they regained consciousness then daily for two days and were single-housed after surgery. Two weeks after surgery, mice were attached to the recording cables and acclimatized to the recording conditions several days. Mice were then recorded for EEG/EMG using a preamplifier (Pinnacle Technology Inc.) connected to a data acquisition system (8200-K1-SE) and Sirenia Software (both from Pinnacle Technology Inc.). Signals were sampled at 400 Hz, digitally filtered (EEG: low-pass FIR filter 30 Hz; EMG: band-pass FIR filter 20–100 Hz). EEG power spectra were computed for 60 s for each behavioral state example by a fast Fourier transform (FFT, Hanning window, 2048 points) routine within the frequency range of 0.25–25.0 Hz.

Resource Table

REAGENT or RESOURCE	SOURCE	IDENTIFIER
Antibodies		
Chicken polyclonal to NF200	Millipore	Cat# AB5539 RRID:AB_177520
Goat anti-Chicken IgG, Alexa Fluor 488 conjugate	Molecular Probes	Cat# A-11039 RRID:AB_142924
Rabbit polyclonal to CGRP	Millipore	Cat# PC205L RRID:AB_2068524
Rabbit polyclonal to PKCγ	Santa Cruz	Cat# sc-211 RRID:AB_632234
Goat anti-Rabbit IgG, Alexa Fluor 488 conjugate	Thermo Fisher Scientific	Cat# A-11008 RRID:AB_143165
Mouse monoclonal to NeuN	Millipore	Cat# MAB377 RRID:AB_2298767
Goat anti-Mouse IgG, Alexa Fluor 488 conjugate	Thermo Fisher Scientific	Cat# A-11001 RRID:AB_2534069
Chemicals, Peptides, and Recombinant Proteins		
Cholera Toxin Subunit B, Alexa Fluor 488 conjugate	Thermo Fisher Scientific	C22841
Fluorescein-conjugated GSL I	Vector Laboratories	Cat# FL-1201 RRID:AB_2314663
Collagenase A	Sigma	10103578001
Dispase II	Sigma	4942078001
Bovine serum albumin	Sigma	A9205-50ml
Neurobasal-A medium	Thermo Fisher Scientific	10888-022
B-27 supplement	Thermo Fisher Scientific	10889-038
L-Glutamine	Thermo Fisher Scientific	25030-081
Penicillin-Streptomycin	Fisher Scientific	MT30001CI
NGF 2.5S native mouse protein	Thermo Fisher Scientific	13257-019
GDNF from rat	Sigma	G1401
Laminin	Sigma	l2020
Poly-D-lysine	Sigma	P6407
Vectashield with DAPI	Vector Laboratories	Cat# H-1200 RRID:AB_2336790
Experimental Models: Organisms/Strains		
Mouse: C57BL/6J: C57BL/6J	The Jackson Laboratory	Cat#JAX000664
Mouse: ChR2-tdTomato: B6.Gt(ROSA)26Sortm27.1(CAG-COP4*H134R/tdTomato)Hze/J	The Jackson Laboratory	Cat#JAX012567
Mouse: TRPV1-Cre: B6.129-Trpv1tm1(cre)Bbm/J	The Jackson Laboratory	Cat#JAX017769
Mouse: Tac1-Cre: B6;129S-Tac1tm1.1(cre)Hze/J	The Jackson Laboratory	Cat#JAX021877
Mouse: Thy1-Cre: FVB/N-Tg(Thy1-cre)1Vln/J	The Jackson Laboratory	Cat#JAX006143
Software and Algorithms		
pCLAMP	Molecular Devices	pCLAMP 10.2
Fiji	Open source	https://fiji.sc
LabVIEW	National Instruments	http://www.ni.com/labview/

Supplemental Reference

Dewachter, I., Reverse, D., Caluwaerts, N., Ris, L., Kuiperi, C., Van den Haute, C., Spittaels, K., Umans, L., Serneels, L., Thiry, E., et al. (2002). Neuronal deficiency of presenilin 1 inhibits amyloid plaque formation and corrects hippocampal long-term potentiation but not a cognitive defect of amyloid precursor protein [V717I] transgenic mice. The Journal of neuroscience: the official journal of the Society for Neuroscience 22, 3445-3453.